FISCHER-TROPSCH SLURRY PHASE PROCESS VARIATIONS TO UNDERSTAND WAX FORMATION: QUARTERLY REPORT, 1 OCTOBER 1988-31 DECEMBER 1988

MASSACHUSETTS INST. OF TECH., CAMBRIDGE

1988

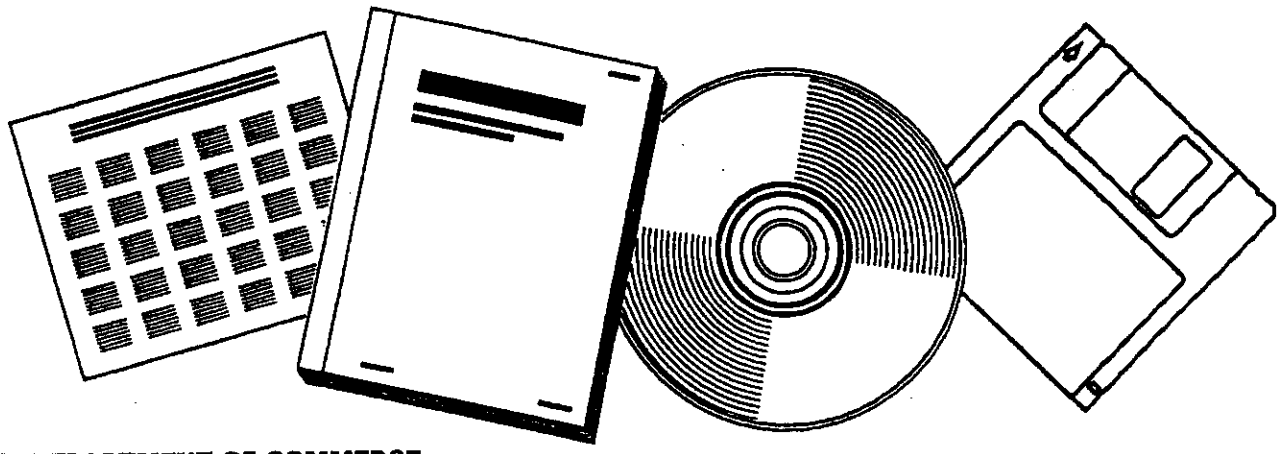

U.S. DEPARTMENT OF COMMERCE
National Technical Information Service

Fischer-Tropsch Slurry Phase Process Variations to Understand Wax Formation

DOE/PC/80015--13

DE89 006704

Quarterly Report for Period

October 1, 1988 to December 31, 1988

Report No.: DOE/PC80015-13

Contract No.: DE-AC22-85PC80015

by

Charles N. Satterfield

for

U.S. Department of Energy

Pittsburgh Energy Technology Center

P.O. Box 10940-MS 920-L

Pittsburgh, PA 15236

Attention: V. Udaya S. Rao

Summary

The effects of temperature and hydrogen/carbon monoxide ratio on carbon number product distribution from iron Fischer-Tropsch catalysts have been studied from recent selected data obtained in our laboratory and from analyses of the literature. These indicate that α_1 = 0.60 - 0.70 for the Schulz-Flory distribution up to about C_{10} for a variety of iron catalysts. α_1 is relatively insensitive to presence or absence of potassium and H_2/CO ratios up to about 10. Values of α_2 for the C_{10+} fraction vary from about 0.89-0.93 at 225°C - 263°C, decreasing to about 0.82 at 310°C.

* * *

Introduction

Numerous studies have been reported on hydrocarbon product distribution from Fischer-Tropsch synthesis on iron catalysts, either in terms of relative amounts of product groups such as wax, diesel fuel, gasoline, etc., or in terms of carbon number distribution. The product composition can vary widely, but it still is not clear to what extent this is caused by the intrinsic kinetic characteristics of the catalyst, such as potassium content, primary versus secondary reactions, the reaction temperature and pressure, (H_2/CO) ratio, or reactor operating characteristics. In many laboratory studies insufficient time has been allowed for the catalyst to reach steady-state activity and selectivity or for the product leaving the reactor to be sufficiently representative of that actually synthesized.

Reports from industrial pilot plant or commercial reactors usually lack information on catalyst composition, and operating conditions are given only in general terms. An example of the wide possible variation in products is seen in the two types of processes used at the Sasol plants in South Africa. Although both use iron catalysts, the entrained bed Synthol reactors produce very little heavy wax and have a high selectivity to gasoline range products, whereas the fixed bed reactors have a higher selectivity to diesel and waxy products. Reactor operating conditions for the fixed bed reactors are in the neighborhood of 220°C (and 2.7 MPa) whereas that for the entrained bed reactors is about 320°C (and 2.2 MPa).

Both catalysts are iron promoted with potassium, but the potassium content may differ somewhat. That used in the Sasol fixed bed reactors is a precipitated catalyst, that in the entrained bed, a fused magnetite. The feed gas composition of the two reactors may also be considerably different. While the Lurgi dry ash gasifiers used at Sasol supply syngas with a H_2/CO ratio of about two[1], the actual H_2/CO ratios to which the catalysts are subjected depend on the reactor recycle ratio and degree of conversion. The H_2/CO usage ratios for iron catalysts are generally much less than two, which means the recycle streams are probably hydrogen-rich. Also, methane from the Synthol reactors is reformed to syngas with a H_2/CO ratio of about 4.5 and fed back to the reactor,[2] thus the reactor H_2/CO ratios may be considerably higher than two.

Experimental Section

The approach of this study was to examine the effects of temperature and feed ratio on one catalyst, a pre-reduced fused magnetite catalyst obtained from Girdler and termed C-73. Its analysis (Galbraith Labs) was 64.4 wt% Fe, 0.76 wt% Al, 0.31 wt% K, and 0.74 wt% Ca, with the remainder oxygen and trace elements. This catalyst is believed to be similar to the fused iron catalyst used in the Synthol reactors.

We have previously reported a series of studies on samples of this catalyst, all taken from the same batch secured by us several years ago[3-9]. Other laboratories have also reported studies with C-73 catalyst, so a mass of data are now available on a base-line catalyst from which useful generalizations can be

drawn. All of our studies have been performed with a continuous-flow mechanically-stirred autoclave in which the catalyst is suspended initially in purified n-octacosane. The methods of operation and analysis have been published.[10-11] The contents of such a reactor are uniform in composition which greatly assists interpretation of data. The overhead exit stream can provide a good representation of products up to about C_{13}. Analysis of pot wax provides further information.

Free Carbon Accumulation. When runs were first attempted at temperatures of about 285-305°C, after about 200 hours on stream temperature gradients began to develop and temperatures varied erratically with time. The cause was finally traced to the buildup of free carbon in the slurry which made the slurry increasingly difficult to mix. The problem was observed at a H_2/CO feed ratio of 0.7, but not at a ratio of 3.8, as might be expected from Dry's correlation of carbon deposition with the ratio $p_{CO}/p^2_{H_2}$.

The free carbon contents of some reactor slurries were determined by taking the carbon and hydrogen analysis of the slurries (by Galbraith Labs) and subtracting the carbon contribution from the hydrocarbons by assuming that all hydrogen came from paraffins with a H/C atomic ratio of two. A correction was made for the contribution of carbon from the catalyst by assuming the catalyst was completely Fe_5C_2, the major phase under Fischer-Tropsch conditions.

The ability of the analytical method to measure iron-bound carbon was tested with the analysis of a sample of cementite,

Fe_3C 99% (Alfa). The result was 7.1 wt% compared to a theoretical value of 6.8 wt%. Our method would include excess surface carbon on the catalyst in the actual slurries, but this would be negligible compared to the quantities of free carbon found. It appears that when the total free carbon content of the slurry reaches about 6 or 7%, the viscosity has increased to such a level or become non-Newtonian so that even a vigorously stirred reactor cannot be kept isothermal. Effective viscosity increases with carbon loading, but also varies substantially with the specific structure of the carbon.[12] Increased viscosity can also be caused by accumulation of wax products, but this was not the major contributor here.

Results: General

Two series of runs were conducted, each series lasting from 300 to 500 hours, during which operating conditions were studied as follows: (1) Runs at 232°C, and various pressures with reactor feed ratios, (H_2/CO), from 5 to 50. (2) Runs at 310°C and various pressures, with reactor feed ratios of 0.7 and 3.8. The consumption (usage) ratio of H_2 to CO over iron is generally about 0.7, so by varying feed rate the percent conversion could be altered and hence the (H_2/CO) ratio in the reactor which, of course, is that actually in contact with the catalyst. From the first series of runs reactor CO/H_2 ratios from essentially zero to about 0.005 were studied. From the second series, reactor CO/H_2 ratios in the vicinity of 0.03 and 1.0 were studied.

Here we report from these runs certain selected results in two categories: 1. composition analyses in the C_3-C_8 range, for

comparison with the performance of the two Sasol reactor types and the Hydrocol reactors, and 2. molecular weight distribution over the entire range of products, for comparison with the products from the U.S. Hydrocol plant operated in the early 1950's and from the Schwarzheide tests performed in Germany in 1943.

Determination of Chain Growth Parameters, α_1 and α_2. It is now well established that two major Schulz-Flory type C-number distributions are observed from most if not all iron catalysts. In most cases the dominating distribution changes at about C_{10}. This is an intrinsic property of the catalyst and is not caused by secondary reactions such as olefin incorporation.[9]

Figure 1 shows a representative Flory plot for the overhead products from a stirred autoclave reactor. There are three regions; the first two are usually modelled with a Schulz-Flory-type distribution using two independent chain growth parameters, α_1 and α_2.[13,14] In region III accumulation of relatively less volatile products in the reactor causes the overhead distribution to drop off from the true product composition with increasing molecular weight. An analogous problem occurs in a fixed-bed reactor associated with liquid accumulation effects in catalyst pores. We have published some theoretical analyses of this effect,[15] also some brief analyses of the time required for a specified percentage of paraffin product of carbon number n to have appeared overhead from an autoclave reactor.[13]

Schulz et al.[16] and Inoue et al.[17] have pointed out that the transition from region I to region II can be quite broad, making

determination of the underlying chain growth parameters difficult. This can be made worse by a narrow region II, limiting the number of representative points.

Quantification of Transition Region. We attempt here to quantify the size of this transition region in order to develop criteria for the interpretation of carbon number distribution data.

Two independent carbon number distributions which follow Flory statistics can be described by the equations,

$$m_{1,j} = m_{1,1}\alpha_1^{j-1} \text{ and } m_{2,j} = m_{2,1}\alpha_2^{j-1} \qquad (1)$$

where $m_{1,j}$ and $m_{2,j}$ are mole fractions at carbon number j, $m_{1,i}$ and $m_{2,i}$ are mole fractions at a reference carbon number i, and α_1 and α_2 are the chain growth parameters. Assume that α_1 is less than α_2. A Schulz-Flory plot of the sum of the two distributions would show the curve,

$$f(j) = \ln(m_1+m_2)_j = \ln(m_{1,1}\alpha_1^{j-1} + m_{2,1}\alpha_2^{j-1}) \qquad (2)$$

The derivative of the curve with respect to carbon number gives the logarithm of the "local" value of the chain growth parameter. The derivative of equation 2 is

$$\frac{d \ln(m_1+m_2)_j}{d j} = \frac{\ln \alpha_1 + (m_2/m_1)_i(\alpha_2/\alpha_1)^{j-i}\ln \alpha_2}{1 + (m_2/m_1)_i(\alpha_2/\alpha_1)^{j-i}} \qquad (3)$$

If we set i equal to the carbon number of the intersection of the two distributions (not necessarily an integer), then (m_2/m_1) is unity. If we also substitute k, the distance from the

intersection, for j-i, equation 3 becomes,

$$\frac{d \ln(m_1+m_2)_j}{d j} = \frac{\ln \alpha_1 + (\alpha_2/\alpha_1)^k \ln \alpha_2}{1 + (\alpha_2/\alpha_1)^k} \qquad (4)$$

By taking the antilog of equation 4, we obtain a formula for the local α,

$$\alpha_{local} = \alpha_1^{\left[\frac{1}{1 + (\alpha_2/\alpha_1)^k}\right]} \quad \alpha_2^{\left[\frac{1}{1 + (\alpha_1/\alpha_2)^k}\right]} \qquad (5)$$

When k is equal to zero, the local α becomes,

$$\alpha_{intersection} = (\alpha_1\alpha_2)^{1/2} \qquad (6)$$

Thus the local effective chain growth probability at the intersection of the two distributions is the geometric mean of the two individual chain growth probabilities.

We now have an expression for the local α as a function of carbon number where the intersection of the distributions is set at zero. The ratio of the local α to α_2 is given by

$$\alpha_{local}/\alpha_2 = (\alpha_1/\alpha_2)^{\left[\frac{1}{1 + (\alpha_1/\alpha_2)^{-k}}\right]} \qquad (7)$$

Figure 2 shows the value of the ratio as a function of carbon number from the intersection for α_1 equal to 0.6 and α_2 equal to 0.9, values which are representative of those observed on the iron catalysts. A similar expression for the α_{local}/α_1

ratio can be written and is plotted in Figure 3. The local chain growth probability is within 10 percent of the asymptotic values after about 2 or 3 carbon numbers, but it takes about 10 carbon numbers for it to come within 1 percent.

Equation 7 can be inverted to solve for the carbon number given the ratios α_1/α_2 and α_{local}/α_2. Equation 8 is the result for $\alpha_{local}/\alpha = 0.9$.

$$k = \frac{\log\left[\frac{\log(\alpha_1/\alpha_2)}{\log 0.9} - 1\right]}{-\log(\alpha_1/\alpha_2)} \qquad (8)$$

Figure 4 is a plot of the number of carbon atoms from the intersection where the local α is within 10 percent of asymptotic value (α_1 in the negative direction and α_2 in the positive), versus α_1/α_2. The representative values of 0.6 and 0.9 for α_1 and α_2 respectively gave a ratio of 2/3 which is near the maxima of the curves. The transition region as defined above is approximately 5 carbon numbers wide. If the intersection for the distributions occurs at C_{10}, which is typical for this catalyst, then care must be taken in reporting chain growth probabilities based on data in the C_7 to C_{13} region. Methane and C_2 hydrocarbons frequently show deviations from the Schulz-Flory distribution so, based on this analysis, we have generally chosen the C_3 to C_7 data here to calculate α_1.

Results and Discussion: α_1 for Light Products

Figure 5 is a plot of α_1 as determined from the C_3 to C_7 products versus CO/H_2 ratio existing in the reactor. The data are from runs with H_2/CO feed ratios from 0.5 to 1.8 (232-263°C,

0.45-1.48 MPa) obtained by Huff[18] to which we have added a set of runs obtained in the present study with H_2/CO feed ratios of 5 to 50, at 232°C, and 0.30-0.79 MPa. Values of α_1 appear to be relatively independent of CO/H_2 ratio, except at very low reactor CO/H_2 ratios.

This relationship is almost linear on a semilog plot, as shown in Figure 6, which corresponds to α_1 being proportional to $n(CO/H_2)^{0.03}$. This may be contrasted to the linear relationship between $1/\alpha_1$ and $(P_{CO})^{-0.3}$ that Schliebs and Gaube[19] reported for a precipitated iron catalyst. Their semi-empirical relationship does not correlate our data, since we observe no dependence on the partial pressures of H_2 and CO as such but only on the ratio.

Dictor and Bell[20] have also reported values of α_1 on the C-73 fused iron catalyst using the C_1-C_7 fraction, from data obtained at 231-285°C and total pressures of 0.3 to 1.3 atm. Their data fall on our correlation, as shown on Figure 7. They correlated their data with an empirical relationship,

$$\frac{(1-\alpha_1)}{\alpha_1} = 0.47 + 0.05\left[\frac{P_{H_2}}{P_{CO}}\right] \qquad (9)$$

Solving for α_1, we obtain

$$\alpha_1 = \frac{1}{\left[1.47 + \dfrac{0.05}{\left[\dfrac{P_{CO}}{P_{H_2}}\right]}\right]} \qquad (10)$$

This function is also plotted on Figure 7. Our data at low CO/H_2 ratios do not fit on their correlation.

The effect of reactor (CO/H_2) ratio on α_1 for five different iron catalysts is compared on Figure 8. The Schliebs and Gaube data[19] were obtained on precipitated iron catalysts, promoted with K or unpromoted, at 260°C and 1.0-1.2 MPa. Their data have the same general trend with CO/H_2 ratio as our data, but the range of CO/H_2 ratios they studied is narrower. The values of α_1 of Schliebs and Gaube, in general, are about 10% lower than our data at the same CO/H_2 ratio. Their values of α were calculated by fitting a two-α model to their data, in contrast to our simple method using the C_3-C_7 range to calculate α_1. If this difference were taken into account, we would obtain very similar values for α_1 for our fused iron catalyst and their promoted and unpromoted precipitated catalysts.

Dictor and Bell[21] studied an unpromoted Fe_2O_3 catalyst (hematite) and a catalyst prepared by adding the Fe_2O_3 to a solution of K_2CO_3 and drying. Reaction conditions were 212-249°C and 2-10 atm. The atomic ratio K/Fe of the dried material was 0.011. In this particular case they reported α_1 on the basis of the C_1-C_3 distribution. These data generally lie higher than ours. This may result from their including C_8 and C_9 in calculating α_1. In Figure 4 of their paper[21] they indicate a break at about C_8 on a Schulz-Flory plot of data from (presumably unpromoted) Fe_2O_3 catalyst. Thus they seem to have included data from the transition region which would increase the influence of α_2 on their calculated values. This would be particularly true

for the potassium promoted catalyst since potassium appears to increase the contribution of products from α_2.[14]

If this factor were taken into account, the difference between our data, the data of Schliebs and Gaube, and the data of Dictor and Bell, would be quite small. This would suggest that the value of α_1 is relatively insensitive to the form or method of preparation of the iron catalysts, or to the presence or absence of potassium within the ranges studied. In the latter respect our conclusions differ from that of Schliebs and Gaube. In their work they attributed the products formed according to the α_1 distribution to unpromoted sites on the catalyst surface.

We find no effect of temperature on α_1 from the fused magnetite catalyst, as shown on Figure 9. This brings together the data of Huff, present studies at 310°C, and present studies at 230°C and high H_2/CO ratios. Dictor and Bell[20] also did not find significant changes with temperature in the range of 248 to 285°C on this fused iron catalyst. They did, however, report that α_1 increases with decreasing temperature on promoted and unpromoted Fe_2O_3 catalysts.[21] This may be an artifact of the carbon number range used to calculate α_1. In the next section, we show that α_2 is greater at lower temperatures. Thus the trend in α_1 observed by Dictor and Bell may have been due to changes in α_2.

Results: Wax Analysis

The products which accumulated in the reactor wax during the runs at 310°C posed a very difficult analytical problem in the determination of the carbon number distribution. An unusually

high density of peaks followed the octacosane peak in the chromatograms from the bonded methylsilicone capillary column used for wax analyses. This multitude of components was not observed at 232-263°C, as shown by the comparison in Figure 10. Treatment of a sample of wax from a 310°C run with hydrogen over a carbon supported rhodium catalyst, yielded no noticeable peak shifts, indicating that the new peaks were probably not olefinic or aromatic in nature. Since these products appeared after the octacosane peak it is probable that these are formed by a reaction with the octacosane carrier, perhaps by some alkylation process.

To eliminate the influence of what appeared to be a secondary process, it was decided to concentrate on the normal paraffins in the waxes which we assumed would indicate the true chain growth probability for the primary products from the catalyst. The run at 310°C with (H_2/CO) = 3.8 feed gas, fortunately produced strong normal paraffin peaks in the chromatograms, allowing for easier identification. Figure 11 shows the results from the two runs at 310°C and one at 234-269°C on the C-73 catalyst. For clarity in presentation the three sets of data are displaced from one another by expressing concentration for each set in arbitrary units. For the lower temperature the α based on C_{33}-C_{43} (except C_{38}) is 0.89.

The data for the two high temperature runs definitely have steeper slopes, indicating lower values of α. Deviations from a linear fit of the data occur here in the C_{28}-C_{32} and C_{36}-C_{39} regions. The former region is affected by impurities as well as

the tail from the octacosane peak in the chromatograms. The latter region is affected by the "crossing" of product peaks through the normal paraffin peaks, that is, a series of product peaks which appear after the normal paraffins early in the chromatogram and gradually end up ahead of the normal paraffins later in the chromatogram. For carbon numbers 36 to 38, the peaks cannot be resolved and thus the normal paraffins appear to be in greater concentration than they actually are. Because of the higher concentration of normal paraffins in the run using $(H_2/CO)_{in}$ = 3.8, this effect was less pronounced than in the run using $(H_2/CO)_{in}$ = 0.7. If the carbon numbers in the above regions are neglected, the alphas for the high temperature runs are about 0.82.

Discussion: α_2 For Heavier Products

Knowledge of α_2 from other studies is more limited because of the difficulty in obtaining representative data in region II. The analysis of the pot wax in the reactor, while it yields a wide range of carbon numbers over which to determine α_2, represents the total accumulated products for all conditions run previous to sampling. Table 1 shows that the range of values of α_2 we have observed from analysis of pot wax for a fused magnetite catalyst in our previous studies in the temperature range 232-263°C is 0.89-0.93.[13,22] Values taken from a number of other reports are also given. The data from the precipitated catalysts used in the Schwarzheide tests are also in about the same range as are results from a proprietary catalyst made by Mobil.

In an early paper Shultz et al.[23] attempted to fit liquid-solid product distribution data form various iron catalysts with that predicted by a single α model. for studies at 200-252°C and 10-15 atm, calculated values of α were about 0.84 to 0.93, but one set gave α = 0.7, from a run at 320-330°C. This last point came from the hot-gas recycle or Michael process which was developed in the late 1930's in Germany.[24] The Hydrocol process, which was also run at high temperature, indicated a value for α_2 of 0.79. Thus an analysis of previous studies indicates a definite trend in α_2 with temperature. A decrease in α_2 would explain at least in part the low wax selectivity from the entrained bed reactors at Sasol.

It should be noted that if reliable data rae available over a wider C-number range, e.g., C_3-C_{15}, α_1 and α_2 can be calculated by a more rigorous statistical technique, discussed elsewhere.[25] However it is more time-consuming to obtain steady-state ddata for products above about C_{10}.[13] The approach here was focussed on comparing data available in the literature which usually report information for light products over a more limited C-number range.

Summary

Our analysis of data available to date suggests that α_1 is relatively insensitive to catalyst composition and operating variables. Values of α_1 = 0.60 - 0.70 encompass a wide variety of iron catalysts, with or without promotion with potassium and at H_2/CO reactor ratios up to about 10.

Less information is available on α_2, but it clearly

decreases significantly with increased temperature. The common observation that increased potassium content increases the average carbon number can be interpreted as increasing the fraction of the total product formed by the mechanism leading to α_2.

TABLE I

EFFECT OF TEMPERATURE ON α_1 AND α_2

	Temperature, °C	α_1	α_2
This study	310[a]	0.65-0.68	$0.82(C_{32}-C_{40})$
	310[b]	0.50-0.55	$0.83(C_{32}-C_{40})$
Huff and Satterfield[13] (see c)	248	0.62	$0.93\ (C_{25}-C_{50})$
Stenger et al.[22]	232-263[d]	--	0.89-0.90 $(C_{25}-C_{50})$
	225-250[e]	--	0.92 $(C_{25}-C_{50})$
Schwarzheide tests[26] (see f)	225 (max.)	0.66-0.69	0.87-0.89
Mobil[26,27] (see g)	255-280	0.66-0.70	0.88
Schliebs and Gaube[19] (see h)	260	0.54-0.65	0.86-0.91
Hydrocol[28] (see i)	315	0.66	0.79
Michael process[23] (See j)	330	--	0.70

[a] $(H_2/CO)_{in}$ = 0.7; 1.48 MPa, fused magnetite. $(H_2/CO)_{reactor} \approx$ 1-2

[b] $(H_2/CO)_{in}$ = 3.8. 1.48 MPa, fused magnetite. $(H_2/CO)_{reactor} \approx$ 40

[c] $(H_2/CO)_{in}$ = 1.81; 0.79 MPa, fused magnetite.

[d] $(H_2/CO)_{in}$ = 0.55-1.8; 0.4 to 1.48 MPa, fused magnetite.

[e] $(H_2/CO)_{in}$ = 1.38; 1.14 to 1.48 MPa, precipitated catalyst containing Cu and K.

[f] Six catalysts were of the precipitated type and contained slightly different K contents. Cu content varied between 1-10 atoms Cu per 100 atoms Fe. One catalyst was fused iron oxide without Cu.

[g] Proprietary precipitated $Fe/Cu/K_2CO_3$ catalyst.

[h] Unpromoted and K-promoted precipitated iron catalysts, (H_2/CO) = 0.6-5.8, 1.0-1.2 MPa. α_1 and α_2 calculated by fitting data to a two-α model.

[i] Alkalized mill scale.

[j] Iron powder treated with potassium borate[24]

References

(1) Massey, L.G. in Coal Conversion Technology, Wen, C.Y.; Lee, E.S., eds., Addison-Wesley, London, 1979, 313.

(2) Dry, M.E., in Catalysis, Science and Technology, Anderson, J.R.; Boudart, M., eds., Springer, 1981, 1, 159.

(3) Huff, G.A., Jr.; Satterfield, C.N. Ind Eng. Chem. Process Des. Dev. 1984, 23, 696.

(4) Satterfield, C.N.; Huff, G.A., Jr.; Stenger, H.G.; Carter, J.L.; Madon, R.M. Ind. Eng. Chem. Fundam. 1985, 24 450.

(5) Stenger, H.G., Jr.; Satterfield, C.N. Ind. Eng. Chem. Process Des. Dev. 1985 , 24, 411.

(6) Stenger, H.G., Jr.; Satterfield, C.N. Ind. Eng. Chem. Process Des. Dev. 1985 , 24, 415.

(7) Satterfield, C.N.; Hanlon, R.T.; Tung, S.E.; Zuo, Z.m.; Papaefthymiou, G.C. Ind. Eng. Chem., Prod. Res. Devel. 1986, 25, 401.

(8) Satterfield, C.N.; Hanlon, R.T.; Tung, S.E.; Zuo, Z.m.; Papaefthymiou, G.C. Ind. Eng. Chem., Prod. Res. Devel. 1986, 25, 407.

(9) Hanlon, R.T.; Satterfield, C.N. Energy and Fuels 1988. 2, 196.

(10) Huff, G.A., Jr.; Satterfield, C.N. Ind. Eng. Chem. Fundam. 1982, 21, 479.

(11) Huff, G.A., Jr.; Satterfield, C.N.; Wolf, M.H. Ind. Eng. Chem. Fundam. 1983, 22, 259.

(12) Satterfield, C.N.; Huff, G.A., Jr.; Stenger, H.G. Ind. Eng. Chem. Fundam. 1981, 20, 666.

(13) Huff, G.A., Jr.; Satterfield, C.N. J. Catal. 1984, 85, 370.

(14) König, L.; Gaube, J. Chem. Ing. Tech. 1983, 55, 14.

(15) Huff, G.A., Jr.; Satterfield, C.N. Ind. Eng. Chem., Process Des. Dev. 1985, 24, 986.

(16) Schulz, H.; Beck, K.; Erich, E. Proc. Methane Conv. Symposium, Bibby, Chang, Howe, Yurchak, eds., Elsevier, Amsterdam, 1987.

(17) Inoue, M.; Miyake, T.; Inue, T. J.Catal 1987, 105, 266.

(18) Huff, G.A., Jr., "Fischer-Tropsch Synthesis in a Slurry Reactor," Sc.D. thesis, Massachusetts Institute of Technology, 1982.

(19) Schliebs, B.; Gaube, J. Ber. Bunseges. Phys. Chem. 1985, 89, 68.

(20) Dictor, R.A.; Bell, A.T. Appl. Catal. 1986, 20, 145.

(21) Dictor, R.A.; Bell, A.T. J. Catal. 1986, 97, 121.

(22) Stenger, H.G., Jr.; Johnson, H.E.; Satterfield, C.N. J. Catal. 1984, 86, 477.

(23) Shultz, J.F.; Hofer, L.J.E.; Cohn, E.M.; Stein, K.C.; Anderson, R.B. Bureau of Mines Bulletin 578, 1959.

(24) Storch, H.H.; Golumbic, N.; Anderson, R.B. The Fischer-Tropsch and Related Syntheses, Wiley, New York, 1951.

(25) Donnelly, T.J.; Yates, I.C.; Satterfield, C.N., Energy and Fuels, in press.

(26) Kuo, J.C.W., "Slurry Fischer-Tropsch/Mobil Two Stage Process of Converting Syngas to High Octane Gasoline," Report, DOE/PC/30022-10 (DE84004411), 1983.

(27) Kuo, J.C.W., "Two-Stage Process for Conversion of Synthesis Gas to High Quality Transportation Fuels," Final Report, DOE/PC/60019-9, 1985.

(28) Anderson, R.B., in Catalysis, Emmett, P.H., ed., Reinhold, 1956, IV, 208.

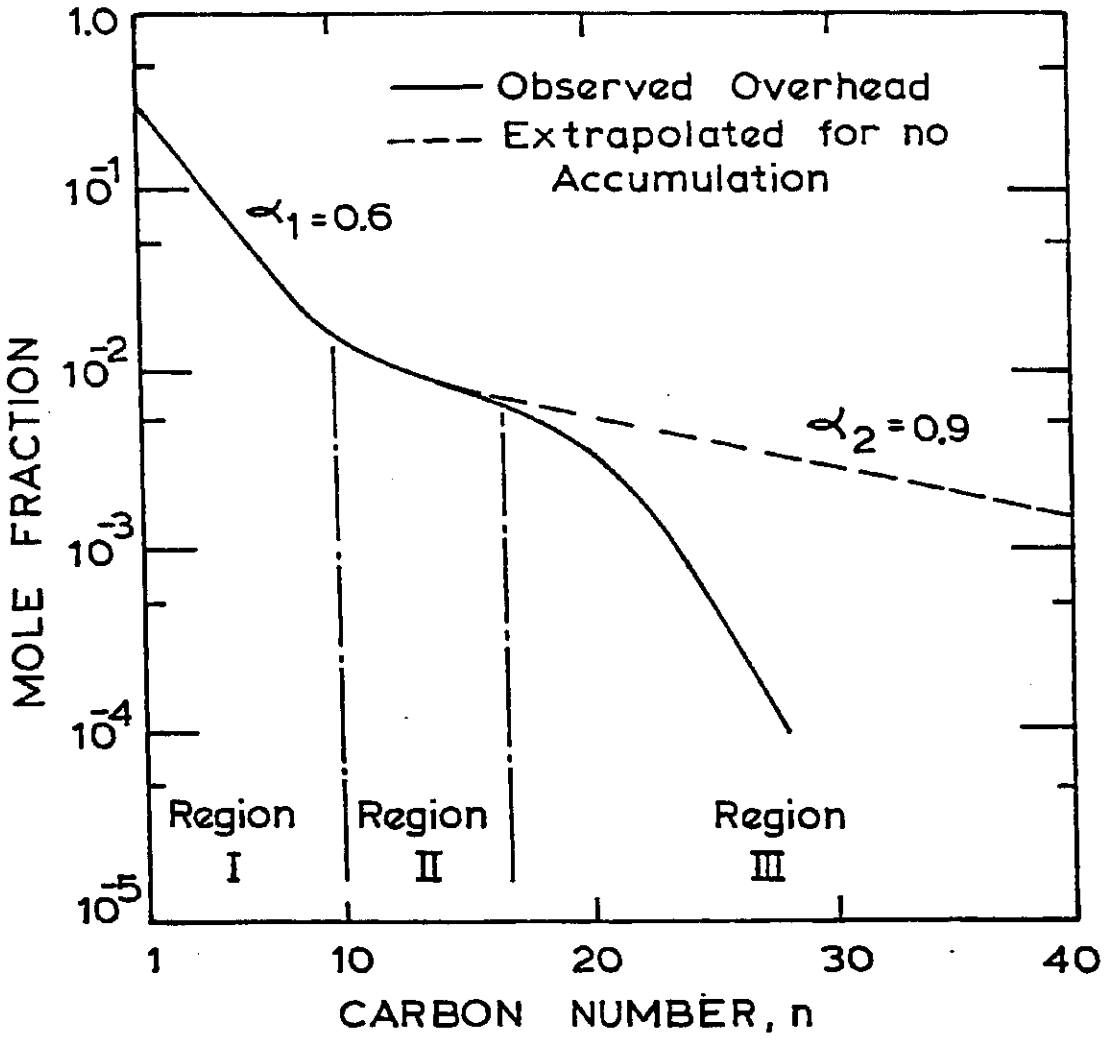

Figure 1: General form of Schulz-Flory plot for reactor effluent from an iron catalyst (after Huff[18]).

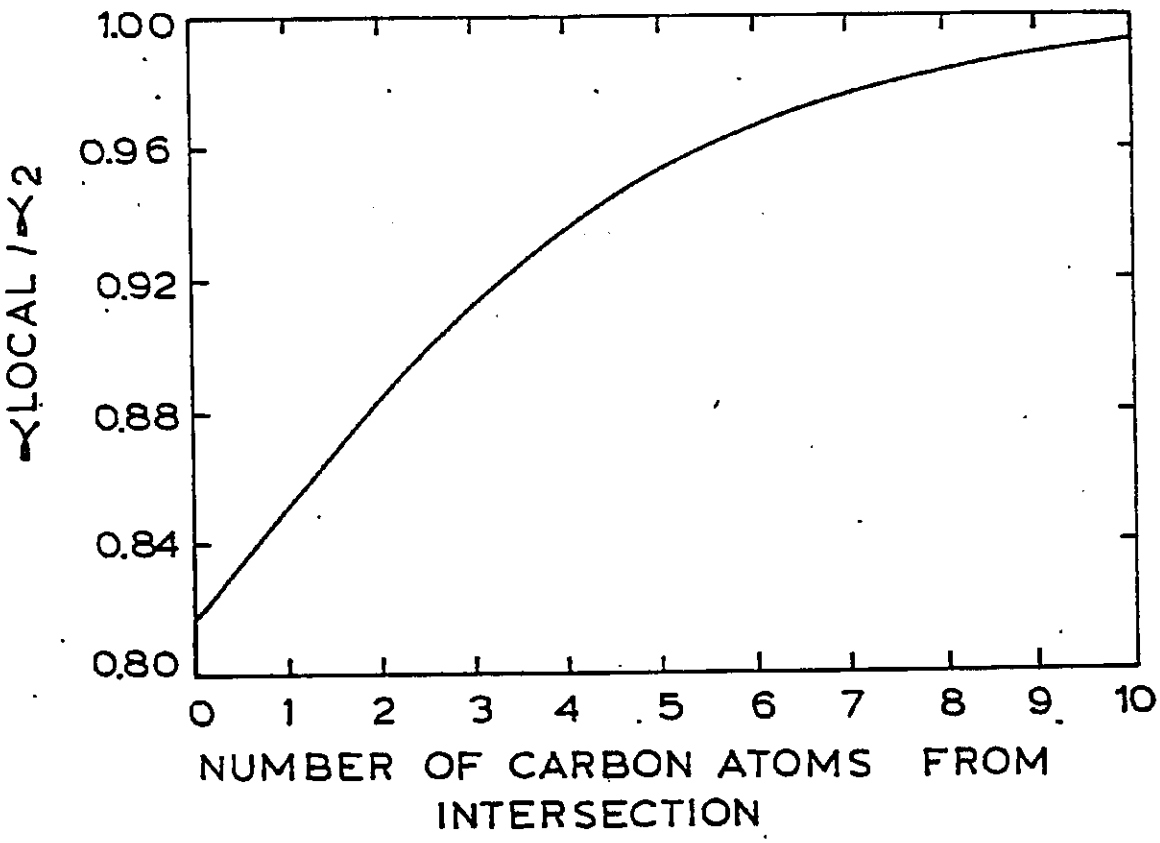

Figure 2: Ratio of α_{local} to α_2 as a function of number of carbon atoms from intersection. $\alpha_1 = 0.6$; $\alpha_2 = 0.9$.

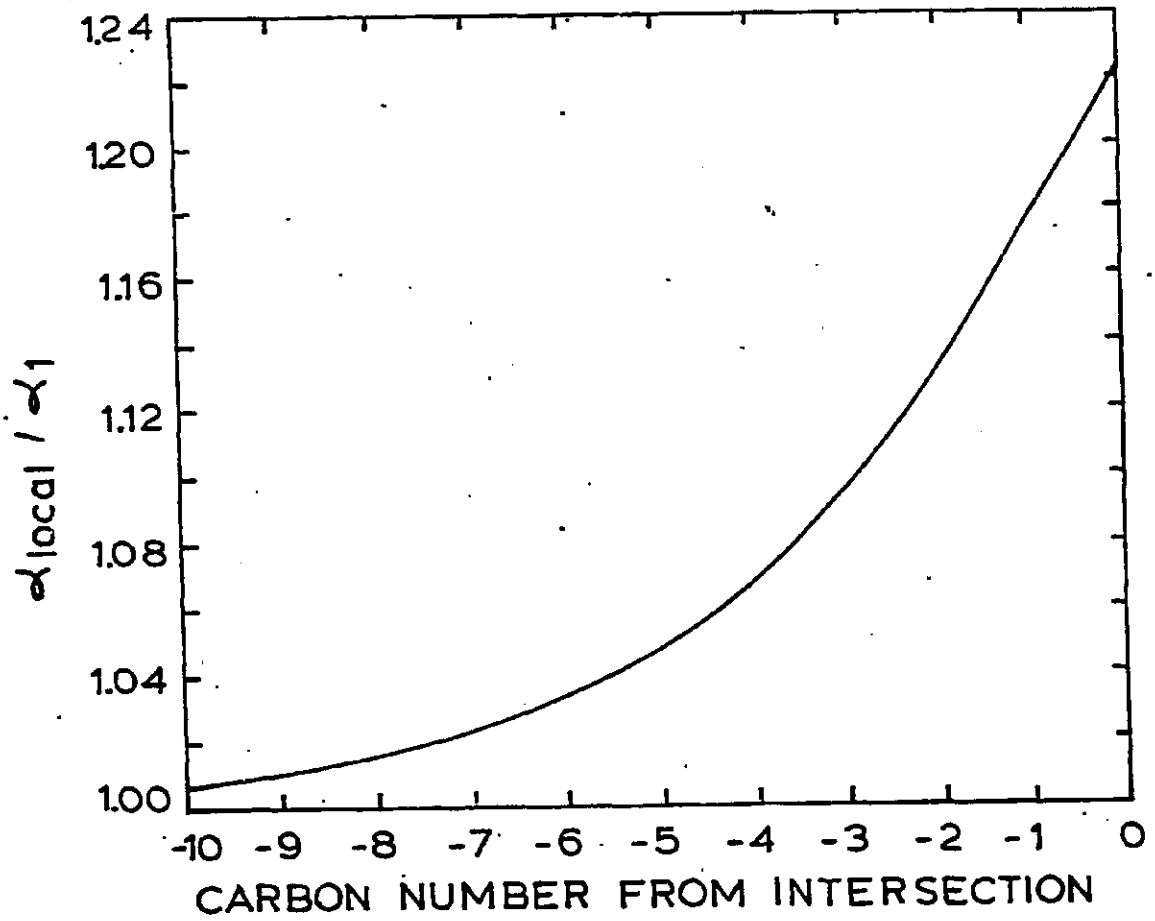

Figure 3: Ratio of α_{local} to α_1 as a function of number of carbon atoms from intersection. $\alpha_1 = 0.6$; $\alpha_2 = 0.9$.

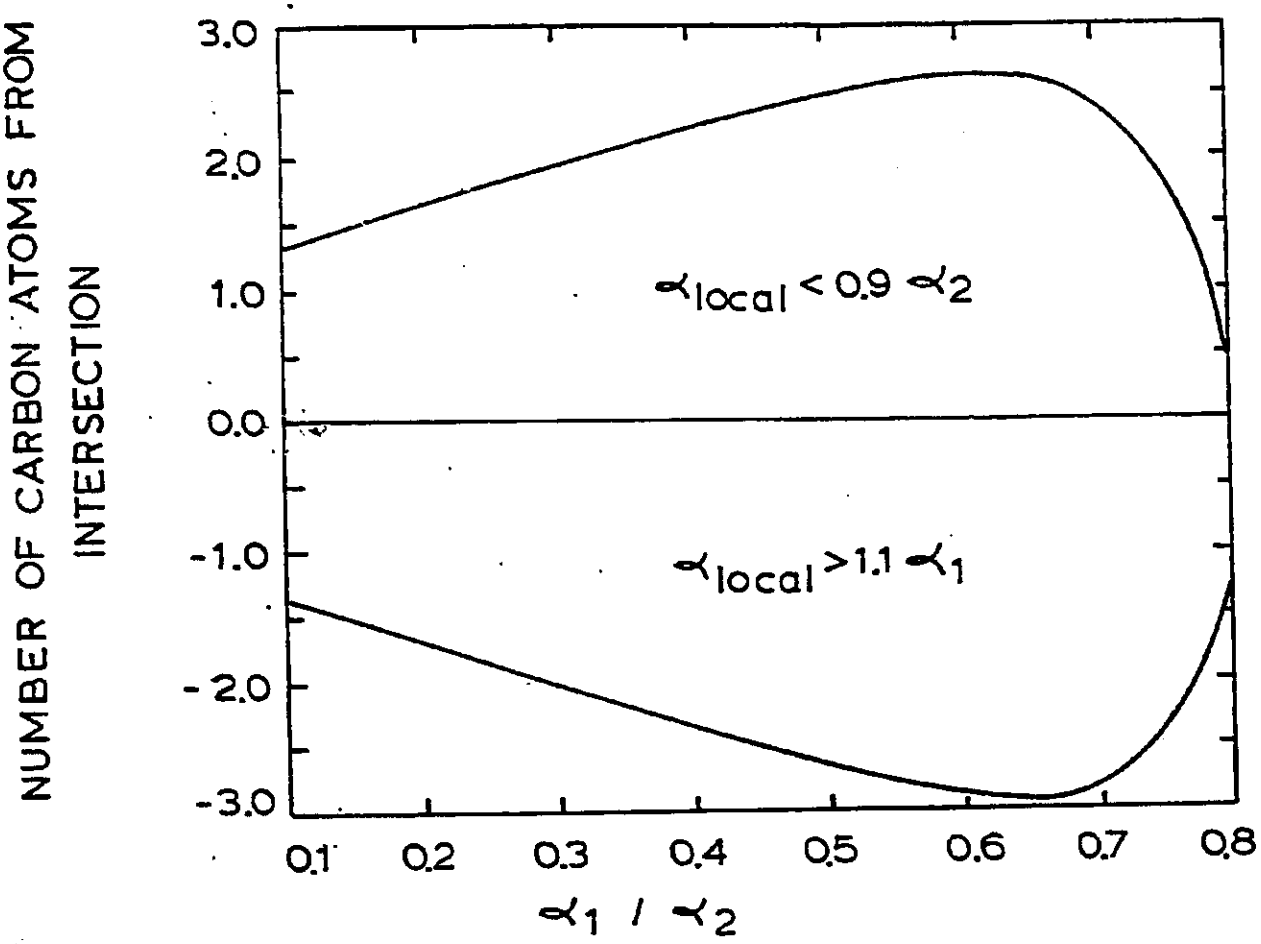

Figure 4 Plot defining regions where α_{local} is within 10 percent of α_1 or α_2.

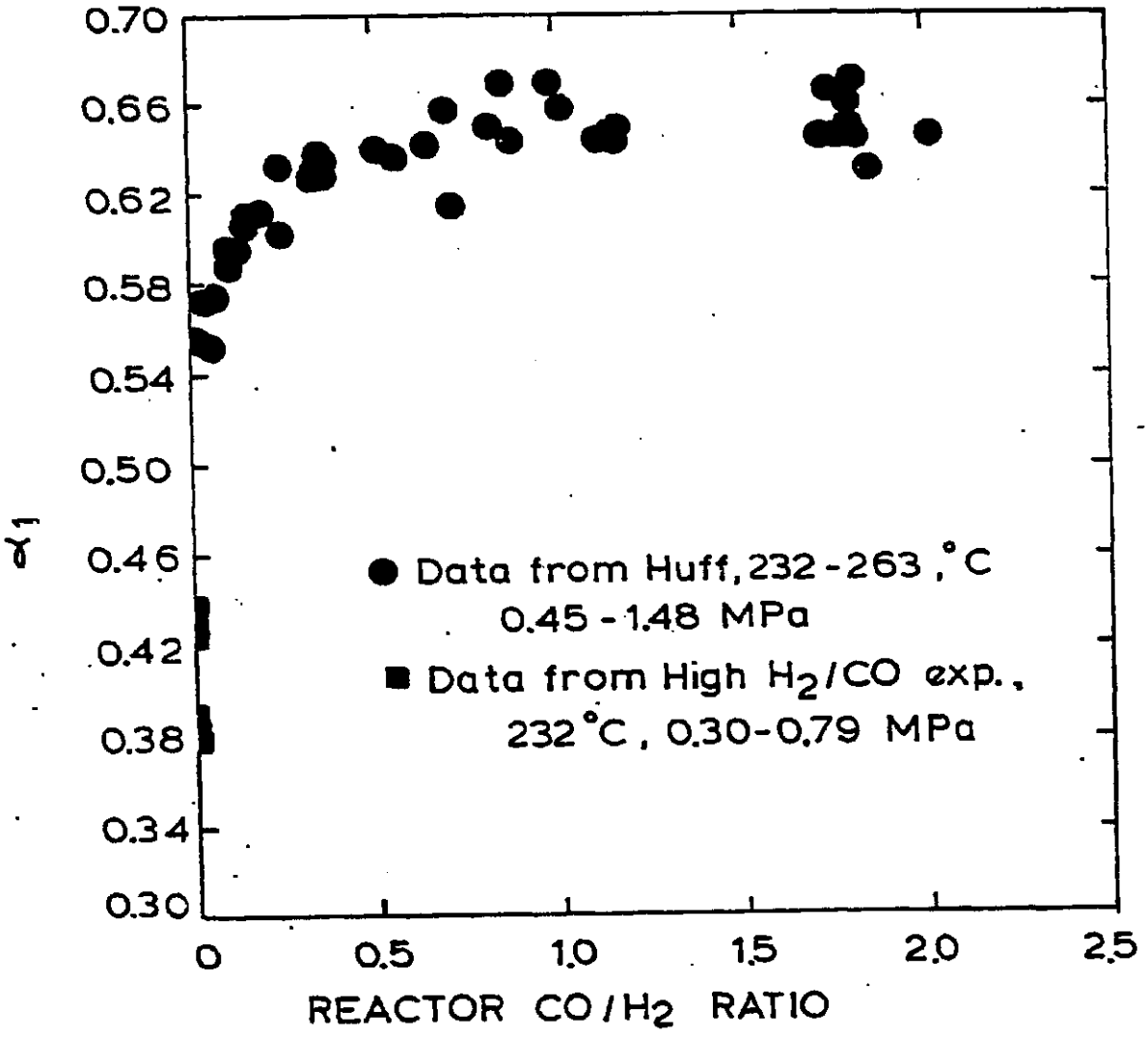

Figure 5 Effect of reactor CO/H_2 ratio on α_1.

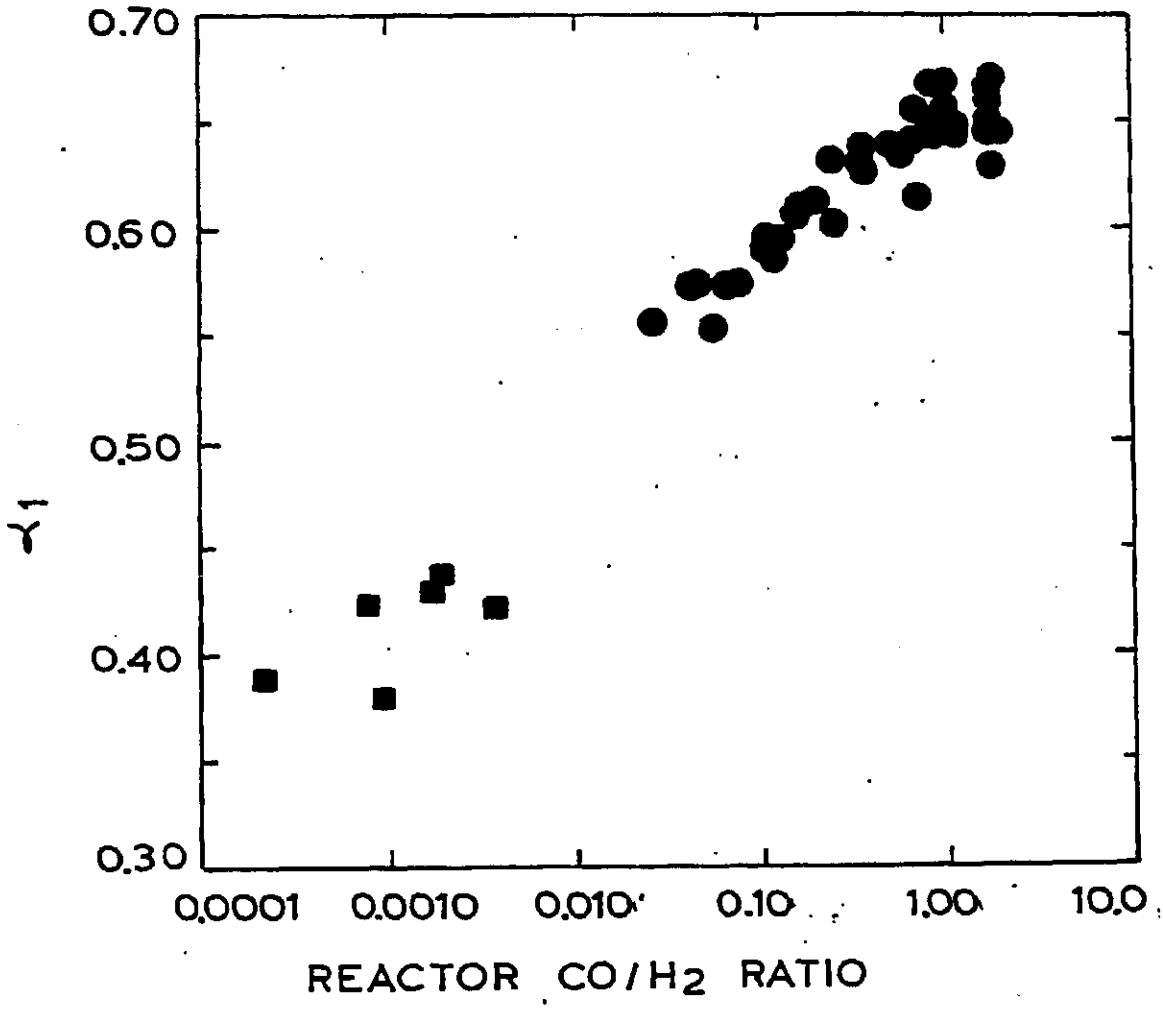

Figure 6 Log plot of abscissa of Figure 5 to separate data at low CO/H_2 ratios.

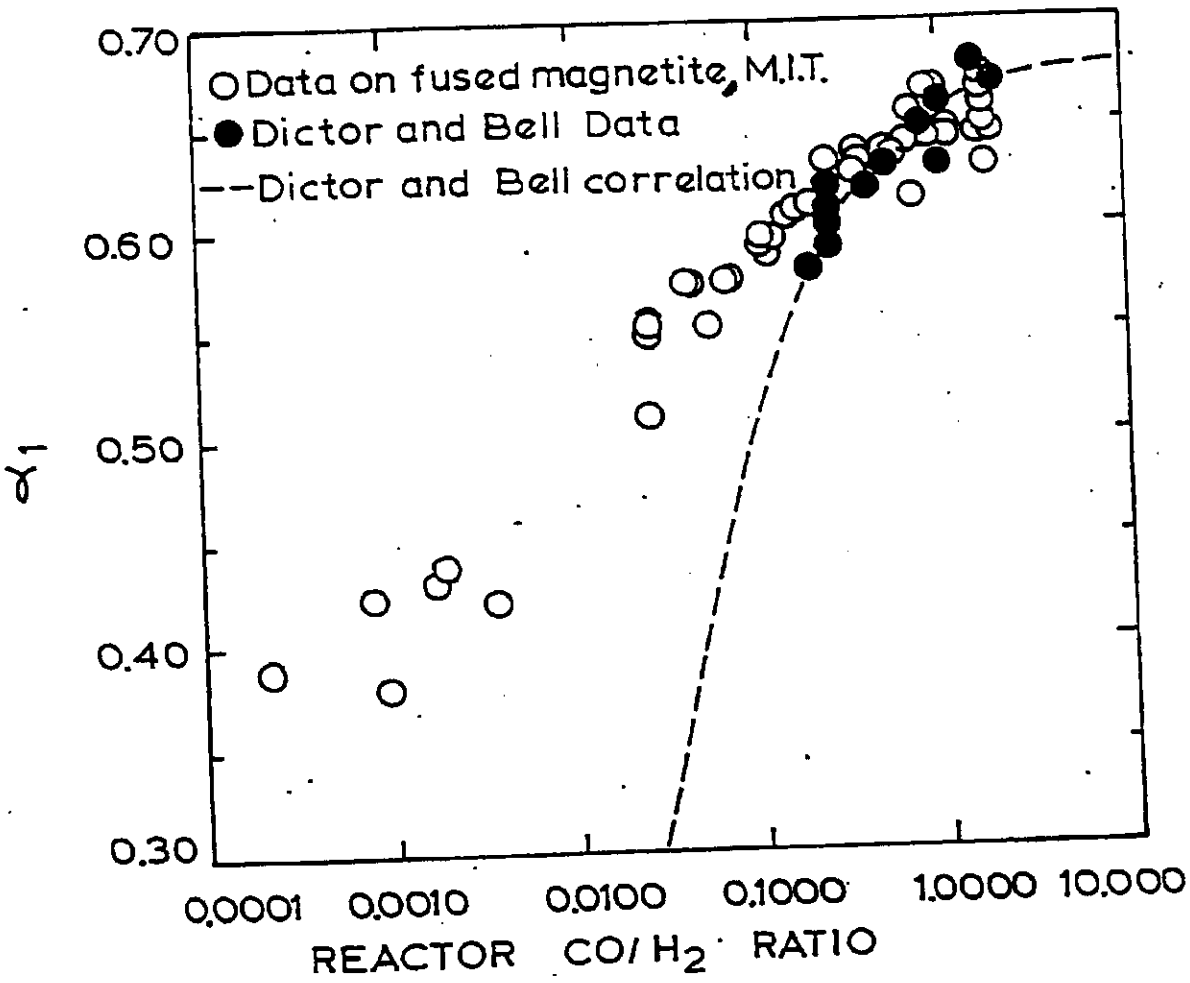

Figure 7 Comparison of present data and that of Huff[18] with data of Dictor and Bell[20], all obtained on fused magnetite catalyst C73.

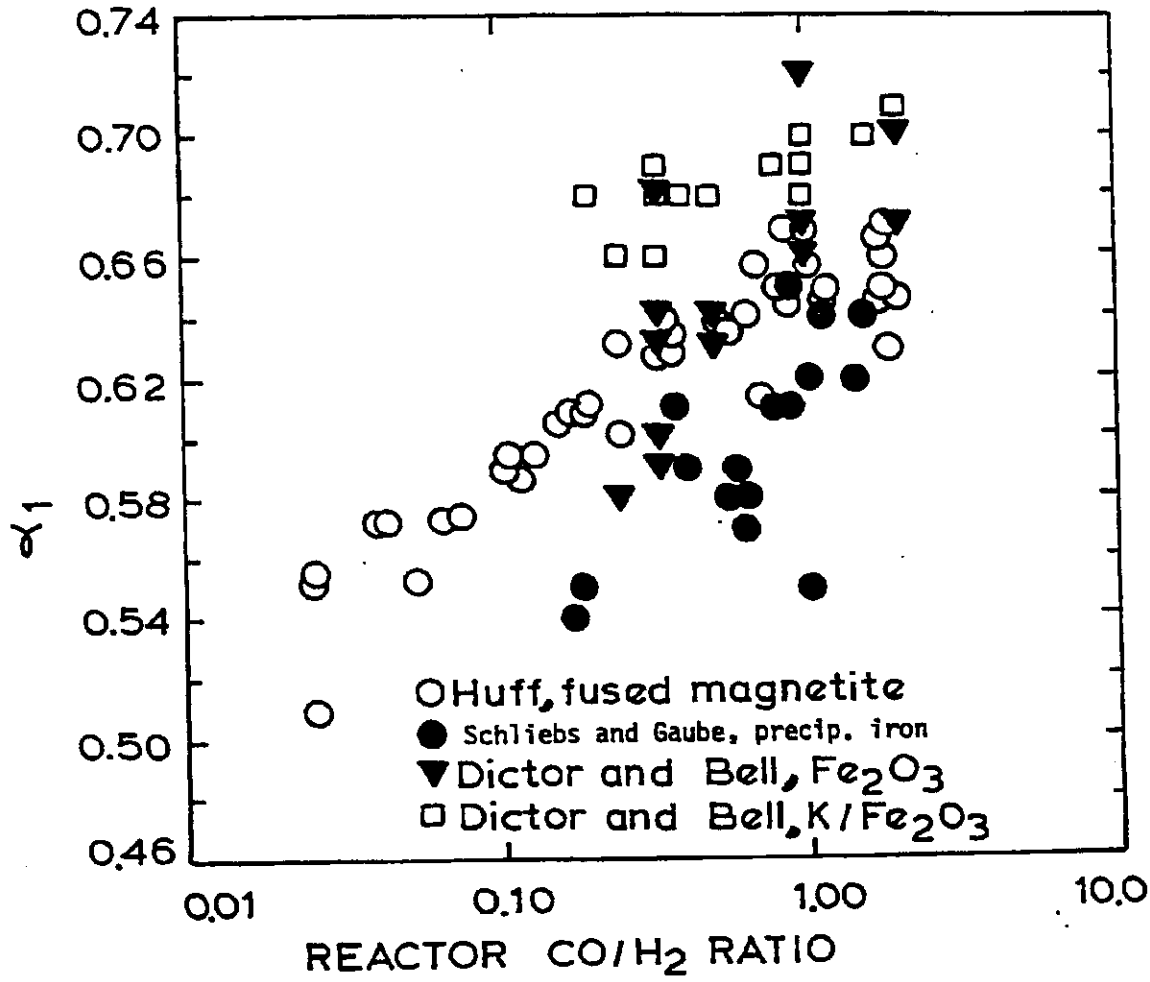

Figure 8 Comparison of α_1 versus CO/H_2 ratio from several iron catalysts.

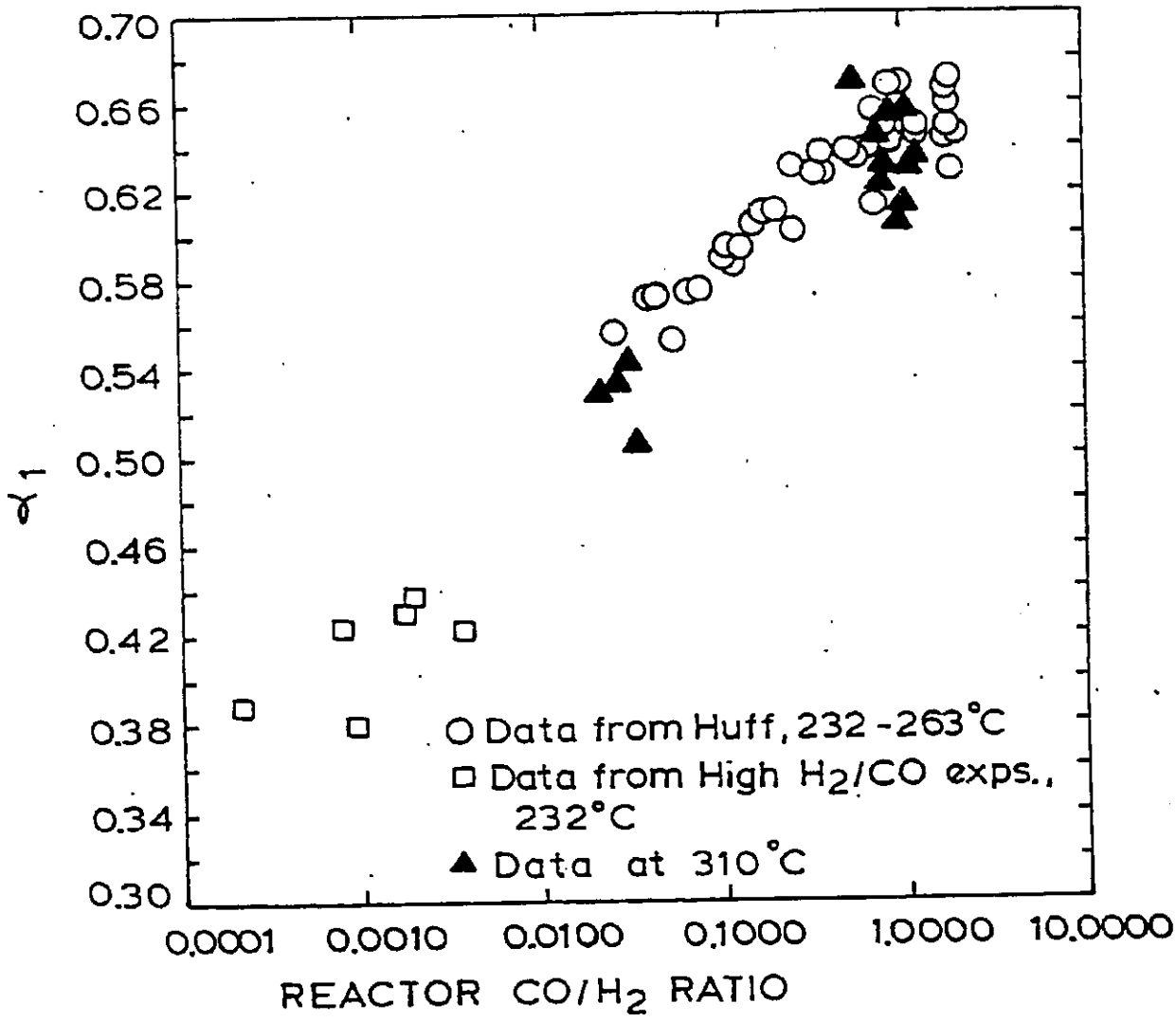

Figure 9 Comparison of α_1 for high and low temperature runs.

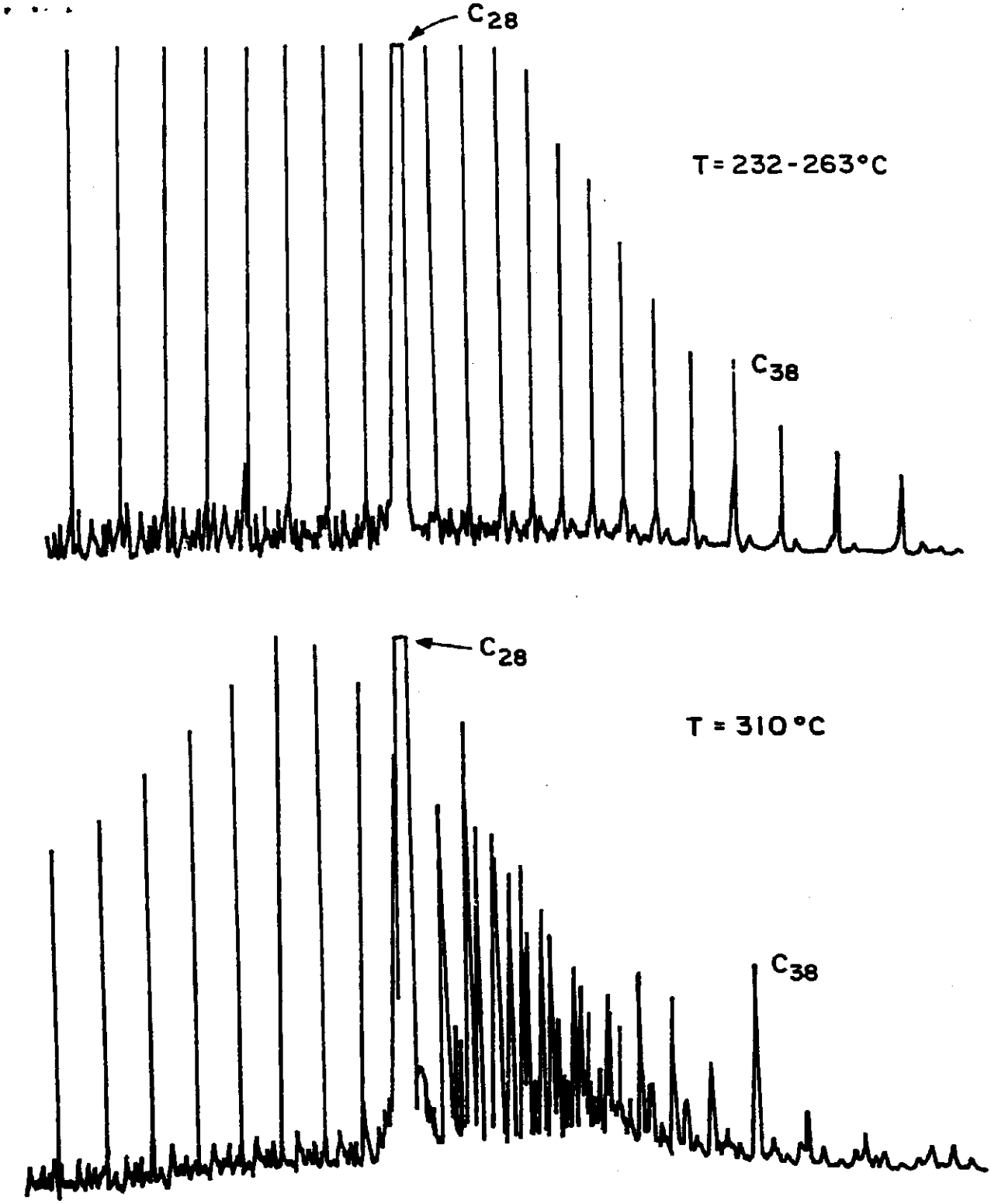

Figure 10 Gas chromatograms for high and low temperature runs.

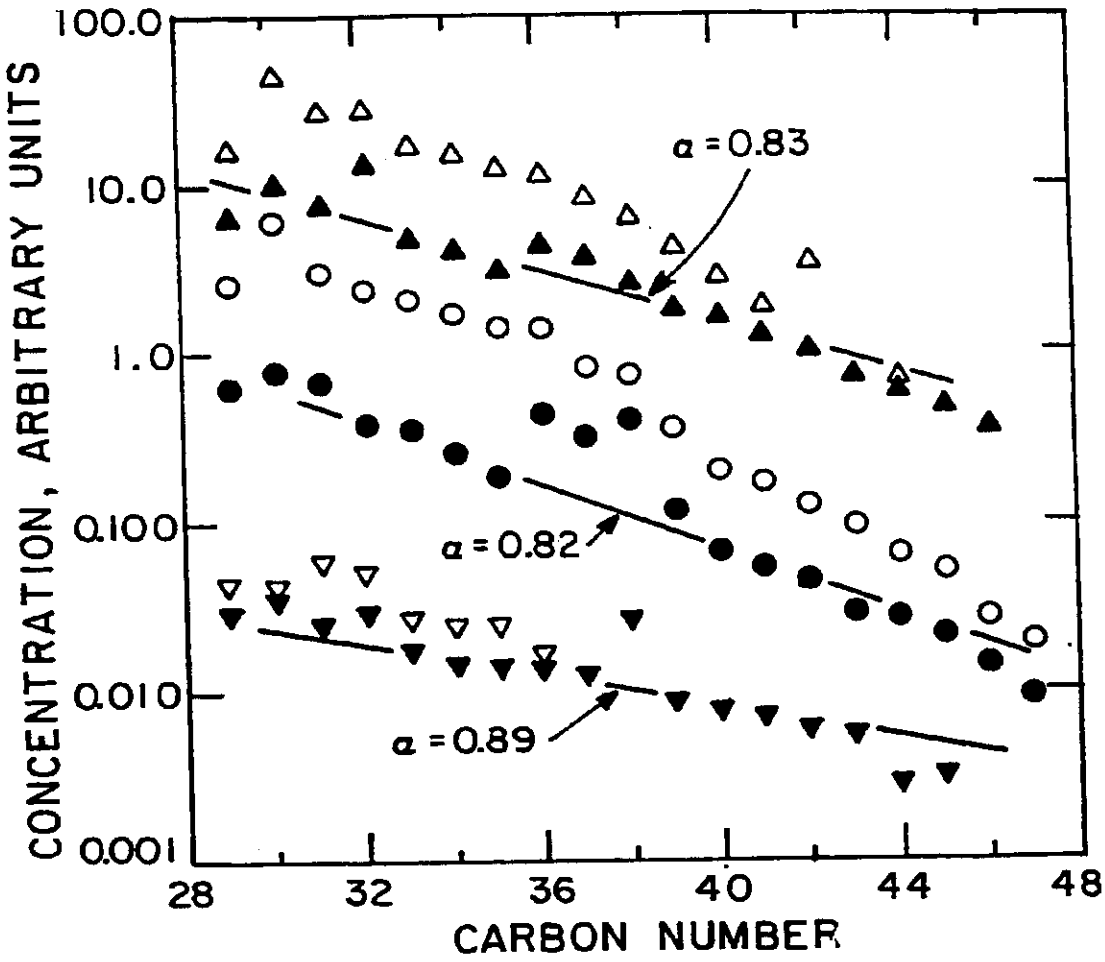

Figure 11 Heavy product analyses from high and low temperature runs.